Electronic Supplementary Material (ESI) for Journal of Materials Chemistry
This journal is © The Royal Society of Chemistry 2011

Supporting Information

Highly Aligned SnO_2 Nanorods on Graphene Sheets for Gas Sensors

Zhenyu Zhang, Rujia Zou, Guosheng Song, Li Yu, Zhigang Chen, Junqing Hu*

State Key Laboratory for Modification of Chemical Fibers and Polymer Materials, College of Materials Science and Engineering, Donghua University, Shanghai 201620, China

* E-mail: hu.junqing@dhu.edu.cn

I. Graphene sheets' preparation

Graphene sheets are prepared using chemical vapor deposition (CVD) method, which was briefly described as following: A ~ 250 nm thick Ni catalyst film was deposited on a Si/SiO_2 substrate using electron beam evaporation. Few-layered, large-area graphene sheets were grown on the thin Ni catalyst coated film using a reaction gas mixture of diluted methane gas source (CH_4:H_2:Ar ~ 50:60:200 standard cubic centimetres per minute) at 1000 °C under ambient pressure in a tube furnace, cooling to room temperature using an Ar flow. Fig. S1 shows the characterization results of graphene sheets.

II. Characterizations

TEM image in Fig. S1a reveals that this as-grown graphene sheet has an area of tens of micrometer square (some even reach more than 100 micrometer square), is multi-layered (≤5 nm, less than 10 layers from the HRTEM imaging, an upper-right inset) and crystalline structure (as revealed by ED pattern, a lower-right inset). The Raman spectrum was dominated by two insensitive peaks at 1332 and 1580 cm^{-1}, which are referred as D line and G line (Fig. 1b), respectively. The G line corresponds to the tangential stretching (E22g) mode of highly oriented pyrolytic graphite (HOPG), indicating the presence of crystalline graphite; the D line is originated from a resonant coupling of the excitation laser with electronic states associated with disordered graphite materials.

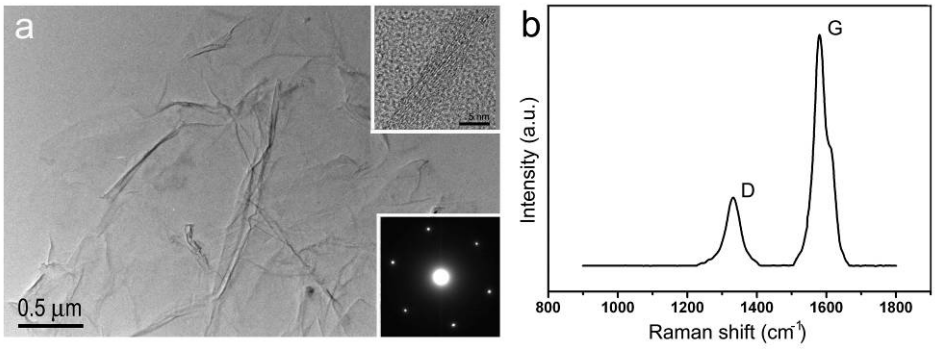

Fig. S1 (a) TEM image of a graphene sheet prepared via a CVD approach, two insets are the corresponding HRTEM image and ED pattern, respectively. (b) Raman spectroscopy of the graphene sheet.

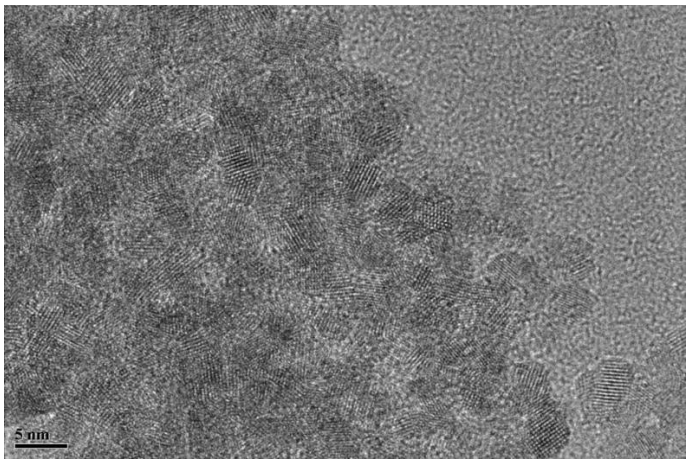

Fig. S2 Higher-magnification TEM image of crystal-seeded graphene sheet. The graphene was experienced hydrolysis of $SnCl_4$ aqueous solution, and calcined at 100 °C for 2 h.

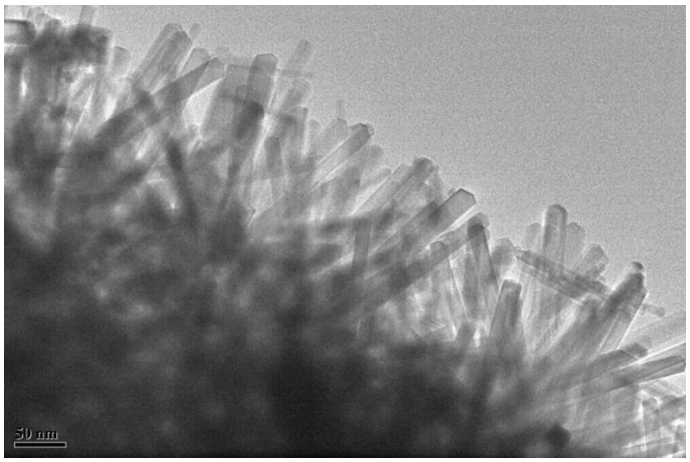

Fig. S3 TEM image of SnO_2 nanorods on Graphene 3-D array strucutures.

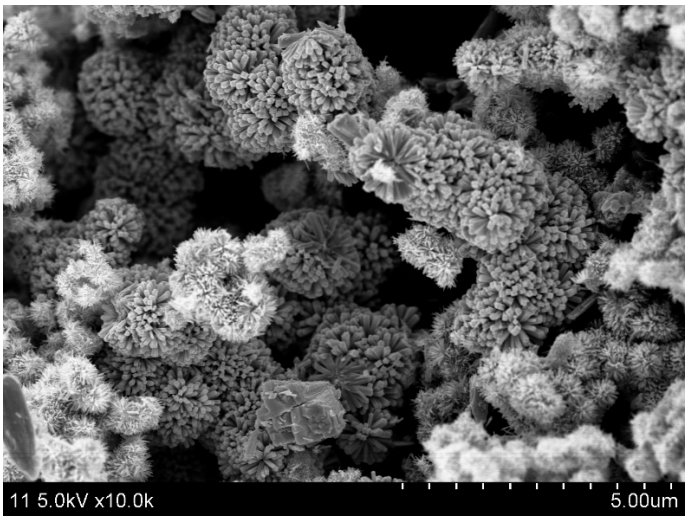

Fig. S4 SEM image of SnO_2 flowers strucutures. If the nanocrystal seeding on the graphene sheets was omitted, the morphology of the product was radial flowers composed with nanorods instead of aligned nanorods array structures.

We have compared the gas sensing performances of the SnO_2/G 3-D nanorod array structures and the SnO_2 nanorods flowers with similar surface area. As exhibited in Fig. S5, the BET surface of the SnO_2/G 3-D nanorods array structures and SnO_2 flower structures is 25.261 and 24.802 m^2g^{-1}, and the average pore size is 3.539 and 3.710 $cm^3g^{-1}nm^{-1}$, respectively. However, the gas sensing response of the SnO_2 nanorod flowers and the SnO_2/G 3-D nanorods array structures to H_2S with a concentration of 50 ppm at 260 ºC is about 60 and 130, respectively, i.e., the former is much lower than the later. So, it is reasonable that the existence of the graphene sheets as SnO_2 nanorod array substrate is an important factor that influences the gas sensing performance, though their surface area and pore size also affect their gas sensitivities.

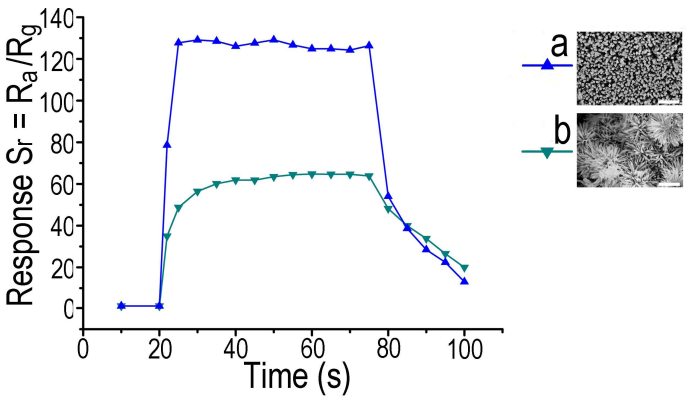

Fig. S5 The dynamic sensitivity of the SnO_2/G 3-D nanorod array structures and the SnO_2 nanorod flowers to H_2S with concentration of 50 ppm at 260 ºC. All scale bars are 500 nm.